General Disclaimer

One or more of the Following Statements may affect this Document

- This document has been reproduced from the best copy furnished by the organizational source. It is being released in the interest of making available as much information as possible.

- This document may contain data, which exceeds the sheet parameters. It was furnished in this condition by the organizational source and is the best copy available.

- This document may contain tone-on-tone or color graphs, charts and/or pictures, which have been reproduced in black and white.

- This document is paginated as submitted by the original source.

- Portions of this document are not fully legible due to the historical nature of some of the material. However, it is the best reproduction available from the original submission.

Produced by the NASA Center for Aerospace Information (CASI)

CORNELL UNIVERSITY

Center for Radiophysics and Space Research

ITHACA, N.Y.

CRSR 646

ASTRONOMICAL POLARIZATION STUDIES

AT RADIO AND INFRARED WAVELENGTHS

PART I

GRAVITATIONAL DEFLECTION OF

POLARIZED RADIATION

A Thesis

Brian K. Dennison

ASTRONOMICAL POLARIZATION STUDIES AT RADIO AND INFRARED WAVELENGTHS

Brian K. Dennison, Ph.D.
Cornell University, 1976

ABSTRACT

In an astrophysical context the polarization of electromagnetic radiation carries important information about the spatial properties of the regions of its origin or those regions through which it has passed. In this thesis two distinct cases are considered.

In Part I the gravitational field is probed in a search for polarization dependence in the light bending. This involves searching for a splitting of a source image into orthogonal polarizations as the radiation passes through the solar gravitational field. This search was carried out using the techniques of very long and intermediate baseline interferometry, and by seeking a realtive phase delay in orthogonal polarizations of microwaves passing through the solar gravitational field. In this last technique a change in the total polarization of the Helios 1 carrier wave was sought as the spacecraft passed behind the sun. No polarization splitting was detected, and the most stringent upper limits are $\approx 5 \times 10^{-8}$ arc seconds. This constitutes a unique confirmation of the equivalence principle. Future work involving compact objects may reveal a polarization dependence in the gravitational scattering of electromagnetic

radiation.

  Part II of this thesis involves possible far infrared polarization of dust clouds. The recently observed 10 micron polarization of the Orion Nebula and the Galactic Center suggests that far infrared polarization may be found in these objects. Estimates are made of the degree of far infrared polarization that may exist in the Orion Nebula. A first attempt to observe far infrared polarization from the Orion Nebula has been carried out. Future observations will be useful in deducing the detailed structure of dust clouds.

BIOGRAPHICAL SKETCH

Brian Kenneth Dennison was born on August 14, 1949, in Louisville, Kentucky, the son of Mr. and Mrs. Kenneth G. Dennison. He has a sister, Sarah.

He received a B.S. with Honors in Physics from the University of Louisville in December, 1970. At Cornell University he received an M.S. in August, 1974 and a Ph.D. in Astronomy in September, 1976. He served as a Teaching Assistant and Planetarium Lecturer at the University of Louisville, and as a Teaching Assistant and Research Assistant at Cornell University. He held Summer Research Assistantships with the National Radio Astronomy Observatory and the Sacramento Peak Observatory.

He was married to Mira Pahlic on July 17, 1976.

ACKNOWLEDGMENTS

The figures were drawn by Mrs. Barbara Boettcher. The final draft was typed by Mrs. I. Marie Jones.

Parts of this thesis were published in the article, "Gravitational Deflection of Polarized Radiation" by Martin Harwit, R. V. E. Lovelace, Brian Dennison, David L. Jauncey, and John Broderick, which appeared in Nature $\underline{249}$, 230 (1974).

TABLE OF CONTENTS

PART I

PART II

LIST OF TABLES

LIST OF FIGURES

PART I

Gravitational Deflection of Polarized Radiation

2

CHAPTER I

GENERAL IDEAS AND THEORY

A.   Introduction

Current theories of gravity predict that orthogonally polar-
ized beams of electromagnetic radiation will be deflected equally by
a gravitational field. Until 1974 (Harwit, et al.) this prediction
had never been tested. A polarization dependent light bending would
be in apparent violation of the Weak Equivalence Principle, i.e.,
the hypothesis that the special relativistic laws of particle kine-
matics are valid in any local inertial frame. If a beam of light
separated into orthogonally polarized beams through the action of a
gravitational field, then when viewed in a freely falling frame at
least one of the beams would follow a curved path in violation of the
special relativistic law for light propagation, ds = 0. (ds is the
differential measure of interval in space-time.)

Viewed alternatively, a stationary observer would note that
oppositely polarized photons follow different trajectories. That is,
the world line of a test particle, in this case a photon, would de-
pend upon its internal state, the polarization. In this way searches
for polarization dependence in the light bending constitute an im-
portant extension of experiments designed to detect variations in
the geodesic motion of test particles of differing internal proper-
ties (Eötvös, et al., 1922; Roll, et al., 1964; and Braginsky and

Panov, 1971). All of the previous experiments have been confined to particles of non-zero rest mass. As elementary particles, photons have few intrinsic properties against which we could search for deviations from null geodesic motion.[*] Of course, the same is true for elementary particles of positive rest mass. However, the Eötvös and subsequent experiments used bulk matter and the various intrinsic properties were superpositions of those of the fundamental constituents. Since different substances were used it was possible to reconstruct the null results in terms of some fundamental properties. For example, it was established that neutrons and protons fall with the same acceleration to a part in 10^{10} (Misner, et al., 1973).

Most modern theories of gravity incorporate the equivalence principle as a fundamental hypothesis. Searching for polarization dependence in the light bending forms a unique test of this basic hypothesis.

At the outset we can make several statements about any polarization dependent bending. Fundamental quantities which might be expected to produce such an effect are the mass of the deflecting body, M, the photon wavelength, λ, the distance of closest approach,

---

[*] It is interesting to note that a special class of energy dependent deviation from null geodesic motion has been sought extensively in the search for photon rest mass. For if the photon has rest mass the geodesics are not null and the energy enters into the initial conditions. Clearly, such a situation does not violate the Weak Equivalence Principle.

b, the angular momentum of the deflecting body, J, and the photon

angular momentum, $\hbar$.[*] Since a differential angular deflection be-

tween orthogonal polarizations is a dimensionless quantity it can

depend only on dimensionless ratios of these quantities (Harwit,

et al., 1973). Intuitively, we might expect some differentiation in

the scattering of orthogonal polarizations whenever ratios such as

λ/M, and λ/b approach unity.

Any splitting of a beam into orthogonal modes as a result of

gravitational bending could conceivably take various forms. The

beam could be split into orthogonal linear polarizations or ortho-

gonal circular polarizations, and the splitting could be parallel

(radial) or perpendicular (tangential) to the gravitational field

gradient. This gives four simple cases: splitting into linear

polarizations in the radial direction (LR), or in the tangential

direction (LT), and splitting into circular polarizations in the

radial direction (CR), or the tangential direction (CT). Certainly

an infinite number of other possible splittings can be imagined,

but they are not considered here because they are not simple. They

do not preserve parallel or perpendicular alignment of the splitting

direction or the fundamental modes of linear polarization with

---

[*] Throughout Part I of this thesis units in which $G = c = 1$ will be used. In these units the mass is equal to GM/c^2 expressed in c.g.s. units, and the angular momentum is GJ/c^3 expressed in c.g.s. units. In particular the solar mass $\simeq 1.5$ km.

respect to the principle axis of the scattering, the radial direction.
Even if such unlikely splittings occur, the would probably show up in
the search for LR, LT, CR, and CT.

These splittings are shown diagramatically in Figure I-1.
Parity conservation can place further restrictions on any possible
splitting (Epstein, 1973). From Figure I-1 it can be seen that under
reflection of the tangential coordinate the splitting direction of
LT reverses. Angular momentum must be represented by a pseudovector,
and under a parity transformation left circular polarization (LCP)
and right circular polarization (RCP) are interchanged. Therefore,
under reflection of the tangential coordinate the splitting direc-
tion of CR reverses. Thus, we see that LT and CR are not parity-
conserving splittings. Indeed, CR would imply that one circular
polarization couples more strongly to the gravitational field than
its orthogonal mode. LT and CR will be included in this discussion
for two reasons: Later in this chapter we shall see that a recent
speculation that gravity is parity-nonconserving implies a small
degree of CR. Also, in the presence of angular momentum in the
deflecting mass (a source of anisotropy in the gravitational field)
LT and CR in general conserve parity. As shown in Figure I-1 LR and
CT conserve parity even in the gravitational field of a nonrotating
mass.

We shall now consider some ways in which polarization depen-
dent bending might occur. Because of the scope of existing

(CR)

(a)

L R
(yes)

L T
(no)

C R
(no)

C T
(yes)
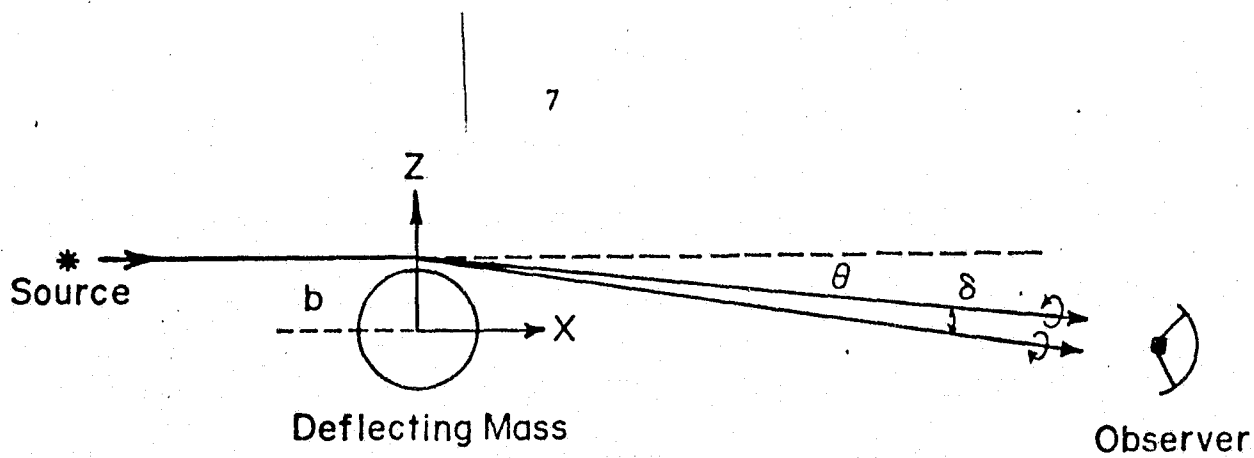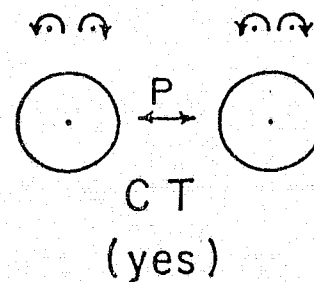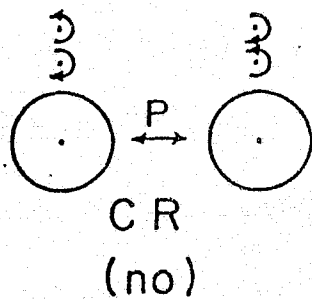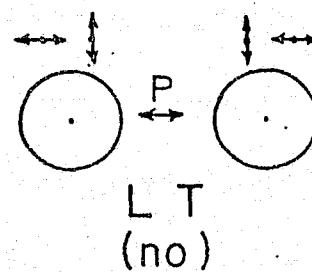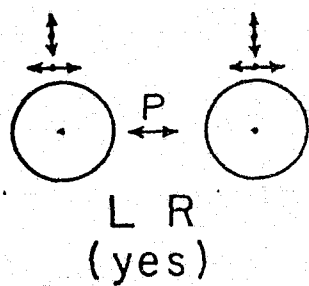
(b)

FIGURE I-1

Polarization splitting by gravitational bending. The general experiment is depicted in (a). The observed image splitting is shown in (b). The effect of coordinate inversion, P, is shown, with the consequences for parity conservation.

experiments (Chapter II) these effects will be discussed primarily in the case of light bending by the sun's gravitational field. In practically all of the cases the predicted splitting will be very small, much smaller than that presently detectable. However, these effects may become important in more extreme cases involving very long wavelengths, strong gravitational fields, and large angular momentum in the deflecting mass (Chapter III). Except when otherwise indicated these effects are not necessarily in viloation of the Weak Equivalence Principle. For example, effects arising because of coupling involving the spatial extent of the photon with inhomogeneities and/or anisotropies in the gravitational field do not meet the local requirements of the Weak Equivalence Principle. In these cases searching for polarization dependence involves a test of gravitation theories beyond the limit of geometrical optics.

B.   Angular Momentum Coupling

It should not be surprising to find that the propagation of radiation is polarization dependent in the gravitational field of a rapidly rotating object. The angular momentum resident in the source imposes an anisotropy on the gravitational field. Because in general relativity the gravitational field is characterized by ten potentials instead of just one, it is possible for the field to contain this anisotropy. Viewed differently, the photon spin couples to the angular momentum of the deflecting mass through the action of the gravitational field. This problem has been treated in some

detail (Mashhoon, 1973, 1974a, 1974b, 1974c, 1975; Skrotskii, 1958; Volkov, et al., 1971). It is possible to analogize this to propagation in an anisotropic inhomogeneous medium. Mashhoon (1973, 1974a, 1974b, 1975) finds that the propagation is governed not just by an effective refractive index, but that a vector potential also arises with the angular momentum as its source. Orthogonal circular polarizations follow separate trajectories, and Mashhoon (1974a) estimates the angular splitting between them to be given by $\delta = \gamma \, \lambda J/b^3$, where γ is a numerical factor expected to be of order unity. For a solar experiment with $\lambda = 3.8$ cm, and $b = 7.8$ $R_\odot$ (Chapter II) $\delta \leqslant 10^{-15}$ milliarc sec (m.a.s.). Such a small effect is not detectable.

For propagation parallel to the source angular momentum vector, the separation angle goes to zero, but the difference in group velocity between orthogonal circular polarizations produces a rotation of the plane of linear polarization. This is analogous to Faraday rotation in an anisotropic medium. This effect has been considered by a number of authors (Balazs, 1958; Mashhoon, 1974a, 1975; Skrotskii, 1958; Volkov, et al., 1971), and is estimated to be of order 10^{-7} arc sec of rotation for radiation passing near the sun.

It might be expected that these effects would be more pronounced for radiation interacting with the galactic gravitational field since the angular momentum is $\sim 10^{22}$ times larger than the solar angular momentum. However, the b^{-3} dependence reduces the galactic effect by the factor $\sim 10^{33}$.

An interesting limiting case in which polarization dependent
effects become extreme involves a maximally rotating black hole
(Shapiro, 1974). Such a black hole can not absorb long wavelength
radiation which would increase its angular momentum per unit rest
mass beyond the limit of maximal rotation. Hence, circularly polar-
ized radiation with spin angular momentum parallel to the hole's
angular momentum can not be absorbed, whereas the orthogonal polar-
ization is readily absorbed.

Another interesting effect has been predicted by Zel'dovich
(1965). He states that radiation emitted deep within the gravita-
tional field of a rotating body undergoes a Zeeman-type splitting.
Viewed from an inertial frame at infinity a gyroscope at radial
coordinate r, rotates with an angular velocity of order $\sim \omega M/r$,
where ω is the rotational velocity of the source mass. Circularly
polarized radiation suffers a shift in frequency in passing to
infinity. This shift is $\sim \pm \omega M/r$ depending upon the alignment of
the photon spin angular momentum with respect to the source angular
momentum. Corresponding to $\sim 1.6 \times 10^{-4}$ rad/sec at the surface of
the Earth, this effect is not observable.

Until now we have been considering the interaction of source
angular momentum with the intrinsic angular momentum of the photon.
However, Corinaldesi and Papapetrou (1951) have considered the simpler
case of a rapidly moving spinning particle in a Schwarzschild (non-
rotating) gravitational field. They find a decrease in the bending

angle of order $\sim \lambda\, M/b^2$, when the particle spin is oriented perpendicular to the plane of motion. For $\lambda \simeq 3.8$ cm near the solar limb this amounts to $\sim 10^{-11}$ arc sec, too small to be detected. For other perpendicular spin orientations, they find no effect on the bending. Of course, if we were to tentatively extend these results to photons (as the authors suggest) we must conclude that the effect for photons is null since the photon spin is colinear with its velocity. It is interesting to note however, that for photons the factor λ/b is just the ratio of spin angular momentum to orbital angular momentum.

C. Coupling with Inhomogeneities in the Gravitational Field

Crawford (1975) has considered the interaction of a photon of finite spatial extent with the gradient of the gravitational field. He predicts a splitting of the type CT, with magnitude of order $\sim \lambda\, M/b^2$. For $\lambda = 3.8$ cm microwaves in the solar gravitational field this amounts to $\sim 10^{-8}$ m.a.s., too small to be detected.

An analogous separation into orthogonal circular polarizations is known to occur when radiation encounters a discontinuity in the refractive index and undergoes total reflection. This is illustrated in Figure I-2. The shift, Δx, is the Goos-Hänchen shift (Goos and Hanchen, 1947), and has been observed experimentally (Goos and Lindberg-Hänchen, 1949). This effect has been reviewed and reanalyzed by Renard (1964). The transverse separation into orthogonal circular polarizations, Δz, was predicted by Costa de Beauregard (1965) and measured by Imbert (1970). This splitting is
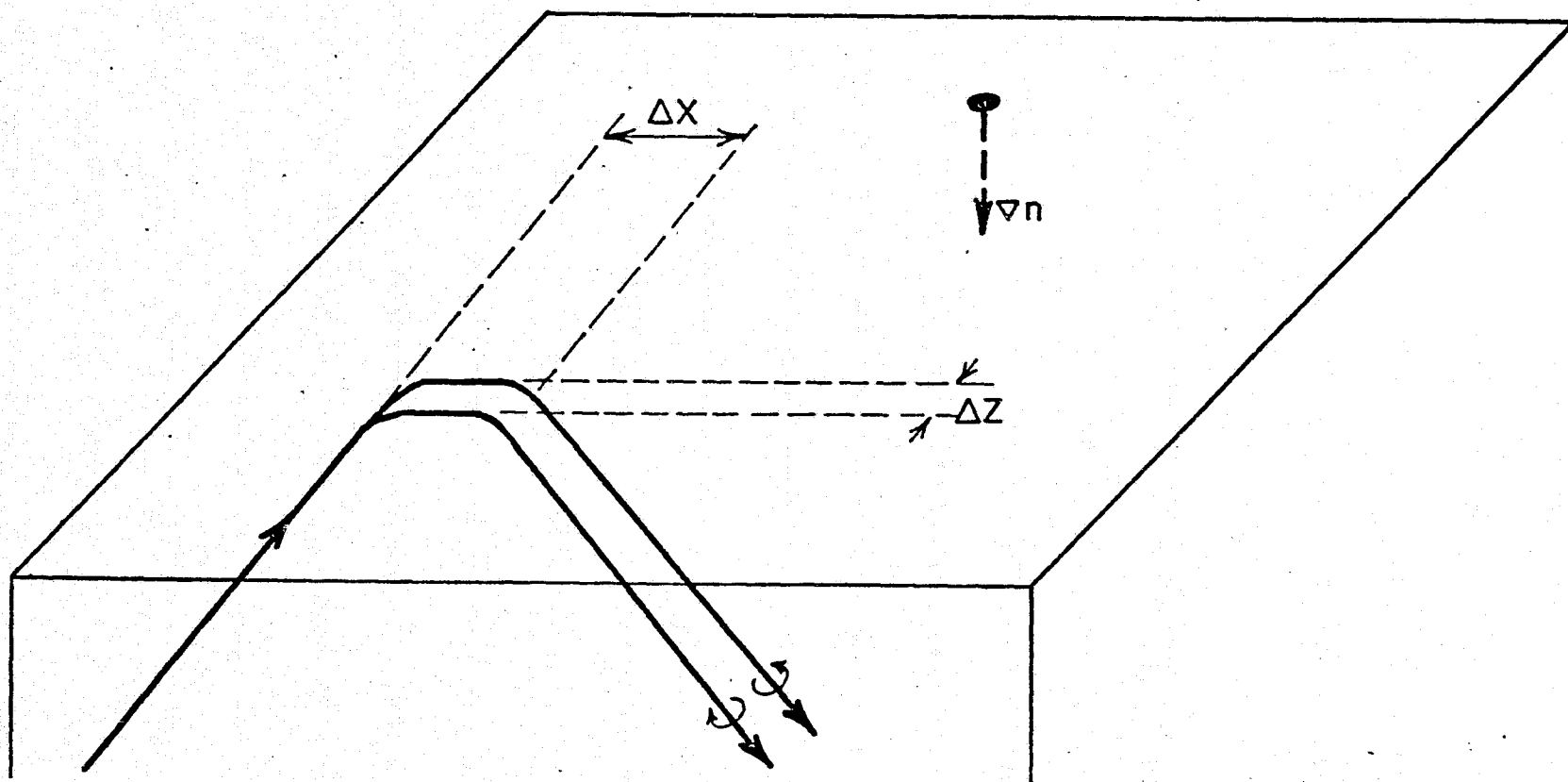
FIGURE I-2

Total internal reflection. The Imbert shift, Δz, splits the beams into orthogonal circular
polarizations.

a consequence of the non-colinearity between photon momentum and
energy flux (Costa de Beauregard, 1965, 1972). Conceivably this
effect might be extended to the gravitational case in which an
effective refractive index varies spatially. However, the change
in the effective refractive index over a wavelength is very small.
Crawford's analysis is different from such an extension. He did
not make use of the non-colinearity between photon momentum and
energy flux.

D.   Parity Nonconservation in Gravitation

Dass (1976a) has recently examined the question of conser-
vation of charge, parity, and temporal invariance in the gravita-
tional interaction. He gives the most general expression for a
C-, P-, T-nonconserving potential in gravitation. In units in
which $G = c = 1$ it is

$$-U_{(r)} = \frac{M}{r} m + \alpha_1 \frac{M}{r} \frac{\vec{S} \cdot \vec{r}}{r^2} + \alpha_2 \frac{M}{r} \frac{\vec{S} \cdot \vec{v}}{r} + \alpha_3 \frac{M}{r} m \frac{\vec{r} \cdot \vec{v}}{r} ,$$

where m is the reduced mass, $\vec{r}$ is the radial displacement of the
scattered particle, $\vec{v}$ is the velocity of the scattered particle,
and $\vec{S}$ is the spin of the scattered particle. Since we are consider-
ing a situation in which the effective mass of the scattered par-
ticle is completely negligible with respect to the mass of the pri-
mary body we can neglect the displacement and velocity of the
primary body. Therefore, symmetrical terms coupling the spin of
the primary body to its displacement and velocity are not included

in the above expression. The dimensionless constants α_1, α_2 and α_3 give rise to C-, P-, T-nonconservation. As α_1, α_2, $\alpha_3 \rightarrow 0$, the Newtonian interaction potential is recovered. In general relativity $\alpha_1 = \alpha_2 = 0$ and $\alpha_3 = 2$. For other values of these parameters there is a breakdown of the equivalence principle.

The effects discussed in Sections B and C are hypothesized to occur as a result of the interaction of the "extent" of the photon with inhomogeneities and anisotropies in the gravitational field. Classically angular momentum involves an assembly of particles nonlocalized in phase space. However, intrinsic quantum mechanical spin is fundamentally different and the extension to this domain is largely untested. Therefore, experiments sensitive to the α- parameters are important tests of the nature of the coupling of intrinsic quantum mechanical spin to the gravitational field (Dass, 1976b).

Dass (1976a) has applied this general potential to gravitating systems involving test particles of nonvanishing rest mass. In particular he finds a cumulative spin precession of $\sim 10^{-6} \alpha_2$ rad per revolution for the binary pulsar (Hulse and Taylor, 1975). Since the period of the binary pulsar is $\sim 1/3$ day the cumulative precession rate is $\sim 3 \times 10^{-6} \alpha_2$ rad/day. Models of pulsar emission invoke synchrotron radiation in a restricted range of angles. The persistence of pulsations from this object over long time periods (~ 1 year) implies $\alpha_2 \lesssim 10^3$.

We now apply the Dass potential to the propagation of photons. Defining $\Phi_{(r)} \equiv \dfrac{U_{(r)}}{m}$ we have

$$\Phi_{(r)} = - \frac{M}{r}\left[1 + \alpha_1 \frac{\vec{\mathcal{S}} \cdot \vec{r}}{r^2} + \alpha_2 \frac{\vec{\mathcal{S}} \cdot \vec{v}}{r} + \alpha_3 \frac{\vec{r} \cdot \vec{v}}{r}\right],$$

where $\vec{\mathcal{S}} = \dfrac{\vec{S}}{m} =$ spin angular momentum per unit mass-energy. For a photon $\vec{\mathcal{S}} = \dfrac{\lambda}{2\pi}\,\hat{s}$, and $|\vec{v}| = 1$, where $\hat{s} = \pm\,\vec{v}$, with the sign depending upon helicity. The identification $\vec{\mathcal{S}} = \dfrac{\hbar}{h/\lambda}\,\hat{s} = \dfrac{\lambda}{2\pi}\,\hat{s}$, for photons is justified since we obtain the same result for a spin-1 massive particle as $|\vec{v}| \to 1$. We then have

$$\Phi_{(r)} = - \frac{M}{r}\left[1 \genfrac{}{}{0pt}{}{+}{-} \frac{\alpha_1}{2\pi} \frac{\lambda}{r} \frac{\vec{v} \cdot \vec{r}}{r} \genfrac{}{}{0pt}{}{+}{-} \frac{\alpha_2}{2\pi} \frac{\lambda}{r} + \alpha_3 \frac{\vec{v} \cdot \vec{r}}{r}\right].$$

We now evaluate the deflection of light predicted by this potential. In the post-Newtonian approximation the equation of motion for a photon is (Weinberg, 1972)

$$\frac{d\vec{v}}{dt} = - 2\,\nabla\,\Phi + 4\vec{v}(\vec{v} \cdot \nabla\,\Phi).$$

It will be assumed that the bending angle is small so that the development of the z-component of $\vec{v}$ can be neglected in integrating the equation of motion. The geometry is shown in Figure I-1. The bending angle is then given by

$$\theta \cong - \frac{\int_0^{V_f} dV_z}{V} = - \int_0^{V_f} dV_z = 2\int_{-\infty}^{\infty} (\nabla \Phi)_z dt = 2\int_{-\infty}^{\infty} (\nabla \Phi)_z dx \ .$$

The second term in the equation of motion does not enter into the calculation since we are neglecting the development of v_z in the integration. In Cartesian coordinates the potential is

$$\Phi = - \frac{M}{\sqrt{x^2+y^2+z^2}} \left[1 \pm \frac{\alpha_1}{2\pi} \frac{\lambda x}{(x^2+y^2+z^2)} \pm \frac{\alpha_2}{2\pi} \frac{\lambda}{\sqrt{x^2+y^2+z^2}} \right. $$

$$\left. + \alpha_3 \ \frac{x}{\sqrt{x^2+y^2+z^2}} \right] .$$

Then

$$(\nabla \Phi)_z = \frac{Mz}{(x^2+y^2+z^2)^{3/2}} \pm \frac{3\alpha_1}{2\pi} \frac{M\lambda xz}{(x^2+y^2+z^2)^{5/2}} \pm \frac{\alpha_2}{\pi} \frac{M\lambda z}{(x^2+y^2+z^2)^2}$$

$$+ 2\alpha_3 \frac{Mxz}{(x^2+y^2+z^2)^2} \ .$$

Along the trajectory $y = 0$, and in the approximation of small bending $z \simeq b$. The integration for the bending angle is

$$\theta = 2Mb \left[\int_{-\infty}^{\infty} \frac{dx}{(x^2+b^2)^{3/2}} \pm \frac{3\alpha_1}{2\pi} \lambda \int_{-\infty}^{\infty} \frac{xdx}{(x^2+b^2)^{5/2}} \pm \frac{\alpha_2}{\pi} \lambda \int_{-\infty}^{\infty} \frac{dx}{(x^2+b^2)^2} \right.$$

$$\left. + 2\alpha_3 \int_{-\infty}^{\infty} \frac{xdx}{(x^2+b^2)^2} \right] .$$

The second and the fourth integrands are odd and thus integrate to zero. The first and third integrals give .

$$\theta = 2Mb \left[\frac{2}{b^2} \pm \frac{\alpha_2}{\pi} \lambda \left(\frac{\pi}{2} \quad \frac{1}{b^3} \right) \right] = \frac{4M}{b} \pm \alpha_2 \frac{\lambda}{b} \quad \frac{M}{b} \; .$$

As $\alpha_2 \to 0$ the general relativistic value for the bending is recovered. The angular splitting is $\delta = 2\alpha_2 \frac{\lambda}{b} \frac{M}{b}$. This splitting is of the type CR, and as expected violates parity conservation. For the bending of microwaves ($\lambda \simeq 13$ cm) at the solar limb $\delta \simeq \alpha_2 \, 10^{-8}$ m.a.s. Applying the limit on α_2 from the binary pulsar $\delta \lesssim 10^{-5}$ m.a.s. This allows the largest splitting yet calculated. As we shall see (Chapter II) this is still below detectability.

The various estimates of possible polarization splitting are summarized in Table I-1. It is interesting to note the apparent importance of the factor λ/b, since the calculated splittings are frequently just the bending ($\sim M/b$) modified by this factor. Clearly we would expect significant splitting whenever long wavelength radiation is scattered with a small impact parameter, and/or when there is large angular momentum resident in the deflecting mass. When the wavelength becomes comparable to the dimensions of the system we are in the domain of physical optics.

TABLE I-1

Theoretical Estimates of the Polarization Splitting

- -

Splitting Mechanism	Splitting Magnitude	Typical Estimate at solar limb (microwaves) (m.a.s.)	References
Angular Momentum Coupling	$\dfrac{\lambda}{b}\dfrac{J}{b^2}$	10^{-15}	Mashhoon, 1974a
Inhomogeneity Coupling	$\dfrac{\lambda}{b}\dfrac{M}{b}$	10^{-8}	Crawford, 1975
Parity Nonconservation	$2\alpha_2\dfrac{\lambda}{b}\dfrac{M}{b}$	10^{-5}	This Work, and Dass, 1976a

PART I

CHAPTER I - REFERENCES

Balazs, N. L., Phys. Rev. 110, 236 (1958).

Braginsky, V. B., and Panov, V. I., Sov. Phys. -JETP. 34, 464 (1971).

Corinaldesi, E., and Papapetrou, A., Proc. Roy. Soc. (London) A,

   209, 259 (1951).

Costa de Beauregard, O., Phys. Rev. 139, B 1443 (1965).

Costa de Beauregard, O., GRG, 3, 391 (1972).

Crawford, D. F., Nature 254, 313 (1975).

Dass, N. D. H., Phys. Rev. Letters 36, 393 (1976a).

Dass, N. D. H., Essay submitted to the Gravity Research Foundation,

   1976b.

Eötvös, R. V., Ann. Phys. (Germany), 68, 11 (1922).

Epstein, R., private communication, 1973.

Goos, F., and Hänchen, H., Ann. Physik 1, 333 (1947).

Goos, F., and Lindberg-Hänchen, H., Ann. Physik 5, 251 (1949).

Harwit, M., Jauncey, D., and Lovelace, R. V. E., Essay submitted to

   the Gravity Research Foundation, 1973.

Harwit, M., Lovelace, R. V. E., Dennison, B., Jauncey, D. L.,

   Broderick, J., Nature, 249, 230 (1974).

Hulse, R. A., and Taylor, J. H., Ap. J. Letters 195, L51 (1975).

Imbert, Ch., Phys. Letters 31A, 337 (1970).

Mashhoon, B., Phys. Rev. D, 7, 2807 (1973).

Mashhoon, B., Nature 250, 316 (1974a).

Mashhoon, B., Phys. Rev. D 10, 1059 (1974b).

Mashhoon, B., Annals of Phys. 89, 333 (1974c).

Mashhoon, B. Phys. Rev. D 11, 2679 (1975).

Misner, C. W., Thorne, K. P. and Wheeler, J. A., Gravitation,
      W. H. Freeman & Co. (1973), pp. 1050-1055.

Renard, R. H., J. Opt. Soc. Am. 54, 1190 (1964).

Roll, P. G., Krotkov, R. and Dicke, R. H., Annals of Phys. 26, 442
      (1964).

Shapiro, S., private communication, 1974.

Skrotskii, G. B., Soviet Phys. Dokl. 2, 226 (1958).

Volkov, A. M., Izmest'ev, A. A., and Skrotskii, G. V., Soviet Phys.
      -JETP, 32, 686 (1971).

Weinberg, S., Gravitation and Cosmology, Wiley & Sons (1972), pp.220-
      222.

Zel'dovich, Ya. B., Pis'ma Letters, Zh. Eksp. Teoret. Fiz., 1, 40
      (1965).

EXPERIMENTS

A.   General Approaches

The measurement of the angle of light deflection by the sun

has been extremely difficult, and highly accurate results have been

obtained only recently (Counselman, et al.,1974; Fomalont and Sramek,

1975, 1976; Weiler, et al., 1975). One reason for this difficulty

is that the apparent angular position of the displaced source must

be compared to sources some distance away in the sky. On the other

hand the search for polarization dependence in the light bending is

quite straightforward. For if there is a polarization dependence

then upon passing behind the sun a source would appear to split

into images in orthogonal polarizations, and one would only need to

measure the separation of the images.

At the present time these experiments are limited to the case

of light bending by the sun. In the future it may be possible to

extend these studies to compact objects.

Two general approaches have been employed in the search for

polarization dependence in the light bending. The first is the

most direct and involves a radio interferometric measurement similar

to that carried out in light bending experiments (Counselman, et al.,

1974; Fomalont and Sramek, 1975). If a source is split into ortho-

gonal polarizations then a systematic fringe phase difference will

result when interferometer fringes obtained in these polarizations are compared. Two experiments of this type were carried out. The first was a very long baseline interferometry (VLBI) experiment. With a baseline of $\sim 10^8$ wavelengths this experiment had intrinsically high angular resolution but suffered from low signal-to-noise ratio. Secondly, fringe phase data from the intermediate baseline ($\sim 10^6$ wavelengths) experiment of Fomalant and Sramek (1975) were analyzed for any polarization dependence. The improved signal-to-noise ratio obtained in this experiment makes it competetive with, or even superior to the VLBI results, despite the shorter baseline. These experiments will be discussed in Sections B and C of this chapter.

A clever alternative to the light bending experiment was proposed by Shapiro (1964). He suggested searching for the delay of light signals which gives rise to the bending. This has been accomplished (Shapiro, 1968). This approach also has its analogue in the search for polarization dependence in the light bending. If orthogonal polarizations are split with a radial component upon passing by the sun then one component must suffer a greater phase delay than its orthogonal mode. This results in a change in the net polarization of the total signal. This technique is by far the most sensitive since it requires a relative delay of only a fraction of a wavelength, whereas the total bending (1.75 arc sec) corresponds to a delay of order 10^5 wavelengths (for 13 cm microwaves) at the

solar limb. This technique also makes optimum use of the relative nature of the measurement. By measuring the final net polarization the relative phase between orthogonal polarizations is measured. This technique is best applied to spacecraft which emit radiation with known Stoke's parameters, and are occulted by the sun.

An experiment of this type was carried out with the Helios 1 spacecraft, and this will be discussed in Section D of this chapter. Also this analysis will be applied to existing data from other space probes.

We now consider the effects that propagation through the solar corona will have on these experiments. To differentially effect the propagation of orthogonal polarizations a source of anisotropy in the plasma is needed. The most obvious candidate is the magnetic field. Rusch and Stelzried (1972) have shown that the quasi-longitudinal approximation is completely adequate for describing the propagation. This means that orthogonal circular polarizations will propagate at different speeds by virtue of their differential interaction with the longitudinal component of the magnetic field. The primary effect of this is to produce Faraday rotation of the plane of polarization. At microwave frequencies Faraday rotation is significant for elongations $\lesssim 7$ $R_\odot$ (Stelzried, et al., 1970; Vollund, et al., 1976). Interferometry experiments searching for LR or LT splitting in this range would be affected. However, the experiments discussed in sections B and C are not

sensitive to linear polarization splitting. Faraday rotation effects

relative phase shift experiments (Section D) in two ways. Firstly,

it mimics CR splitting, and in a single frequency experiment it can

not be separated from any gravitational effect. Secondly, in

searching for LR splitting, Faraday rotation is useful, since it

can produce radiation polarized at 45 degrees at closest approach,

the optimum condition for LR splitting.

Separation of the trajectory into orthogonally polarized

beams (plasma birefringence) would probably be very small. Such an

effect would tend to mimic the gravitational effect sought. If no

splitting is observed, then we can rule out birefringence from any

source (gravitational or plasma). It is highly unlikely that plasma

birefringence and gravitational birefringence could conspire so as

to cancel over a large range of solar elongation angle.

Another anisotropy will be present if the plasma is stream-

ing with relativistic velocity (Lusignan, 1963). This comes about

because of the difference between the longitudinal and transverse

mass of the electron. For radial streaming, radiation polarized

radially and tangentially would propagate at different speeds.

Radiation initially polarized at 45 degrees would undergo a tran-

sition to circular polarization. As we shall see (Section D) this

is identical to the change of polarization produced by LR splitting

For typical solar wind velocities ($\sim$ 400 km sec^{-1}) this effect is

negligible. A null result in LR splitting can be interpreted as a

lack of both gravitational and streaming effects.

Finally, we should make note of the capabilities of the two experimental approaches. While the relative phase shift technique is by far the more sensitive, it is limited to radial splitting. Interferometry can be used to test for all conceivable splittings. Therefore, development of both methods is important.

B.   Very Long Baseline Interferometry

To search for any polarization splitting with high angular resolution VLBI was used in a first attempt. As we are only searching for a relative displacement, the quantity to be measured is the relative phase difference orthogonal polarizations as the source is observed through the sun's gravitational field. This is independent of local oscillator phase at each site, and in this way we can make use of the full resolution of the interferometer.

The observations were carried out with the Green Bank-Owens Valley baseline on September 30 (day 274) and October 4 (day 278), 1972, when the radiation from 3C 273 and 3C 279 passes near the solar limb. The baseline is 3900 km (10^8 wavelengths) and is nearly east-west. The Mark II VLBI tape recording system was used. The observations in Green Bank were carried out with the Howard E. Tatel 85-foot (85-1) radiotelescope of the National Radio Astronomy Observatory (NRAO), and the frequency standard was obtained from the hydrogen maser installed at the 140-foot dish. At the Owens Valley Radio Observatory (OVRO) both A and B 90-foot radiotelescopes

were used, and a Sulzer crystal oscillator, phase locked to a Hewlett Packard 5065A frequency standard, was used. Synchronization was obtained from Loran C radio transmissions at NRAO and from the Goldstone Tracking Station at OVRO. The overall VLBI system is shown schematically in Figure II-1.

Different polarizations were sampled by switching 85-1 between LCP and RCP every 2 sec, while switching between antennas A and B at OVRO every 1 sec. Antennas A and B had linearly polarized feeds, which were preset to be orthogonal. Hence, in 4 sec period all four combinations of polarization were sampled. (Figure II-2.) As the coherence time of the rubidium-driven Sulzer oscillator is much longer than the switching rate, relative phases between the different polarizations were easily obtained. The preliminary reduction was accomplished with the NRAO Mark II processor, and the fringes corresponding to the various polarizations were sorted by computer and combined into their respective groups. The VLBI interferometer was sensitive to dual sidebands of 2 MHz width centered at 8075 and 8095 MHz. Each sideband was processed separately.

In Figure II-3 the relative positions of 3C 273, 3C 279, and the sun during the experiment are shown. Unfortunately, the signal-to-noise ratio for 3C 279 was too small to allow us to make any convincing measurements of relative phase, although weak fringes were detected. This is due to the weak correlated flux (Kellerman, et al., 1974) in 3C 279 ($\leqslant$ 3 f.u.). The correlated flux in 3C 273 was about

FIGURE II-1

The VLBI system.

$$\Delta \phi = 2\pi \frac{b}{\lambda} \sin \theta$$

OVRO 90'
Antennas

NRAO 85'-1
Antenna

$b \approx 3900 \text{km}$

Switch

Switch

RF

RF

Local
Oscillator

Mixer

Mixer

Local
Oscillator

Rubidium
Oscillator

IF

IF

H-Maser
Oscillator

Clock

Tape
Recorder

Tape
Recorder

Clock

Playback

N R A O
Correlator
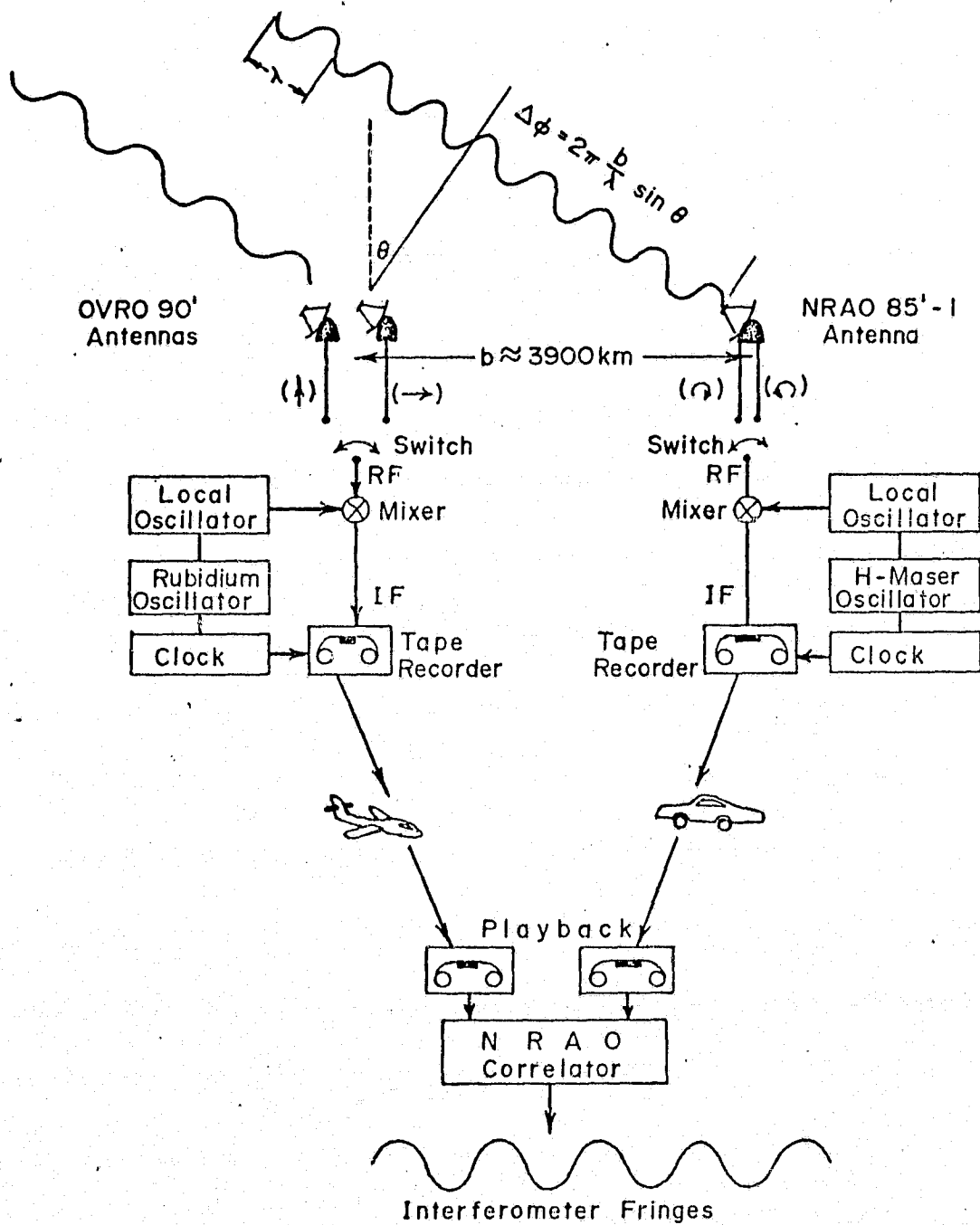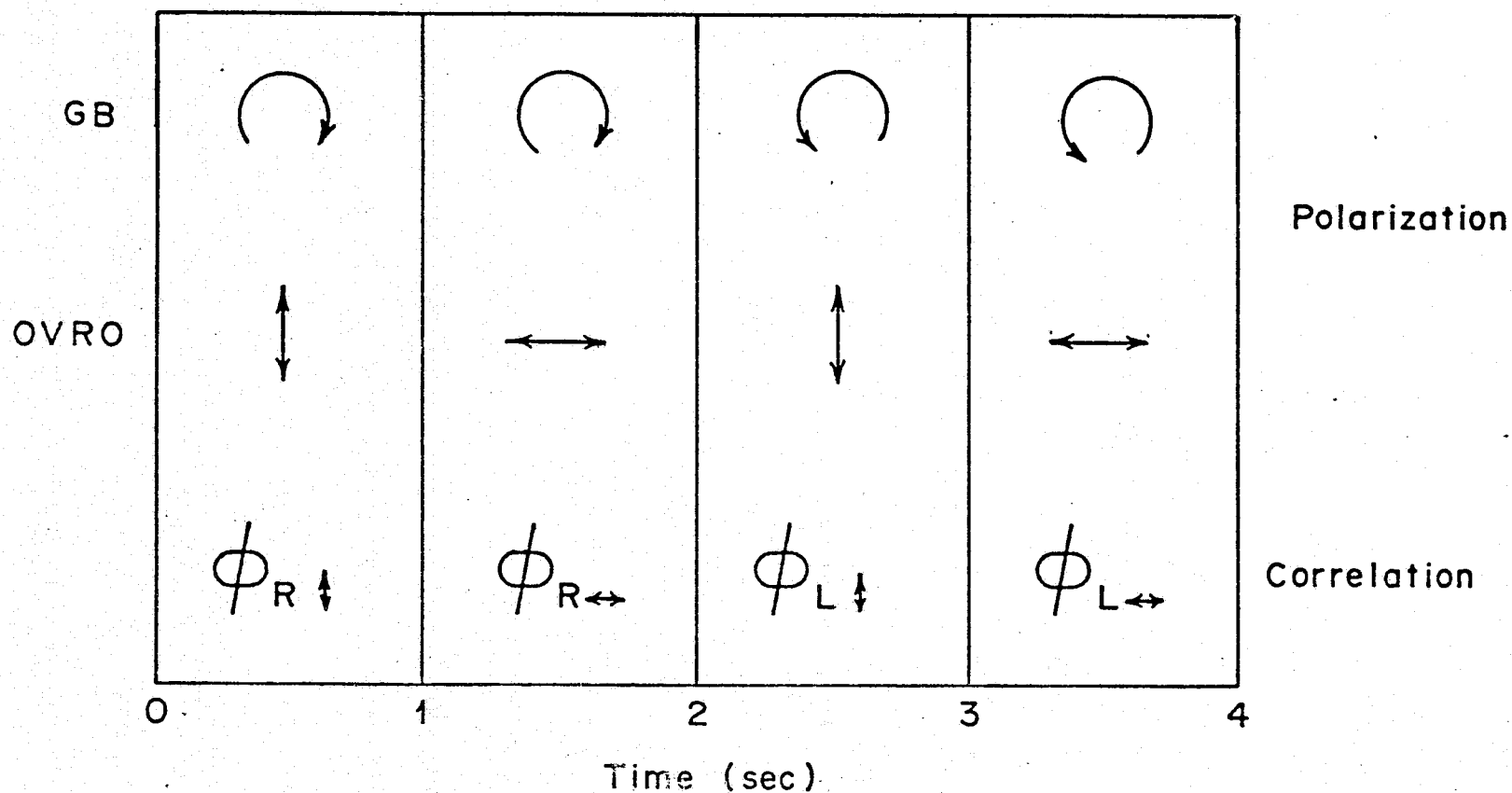
Interferometer Fringes

FIGURE II-1

FIGURE II-2

Polarization switching scheme. In a four second period all combinations of polarization were
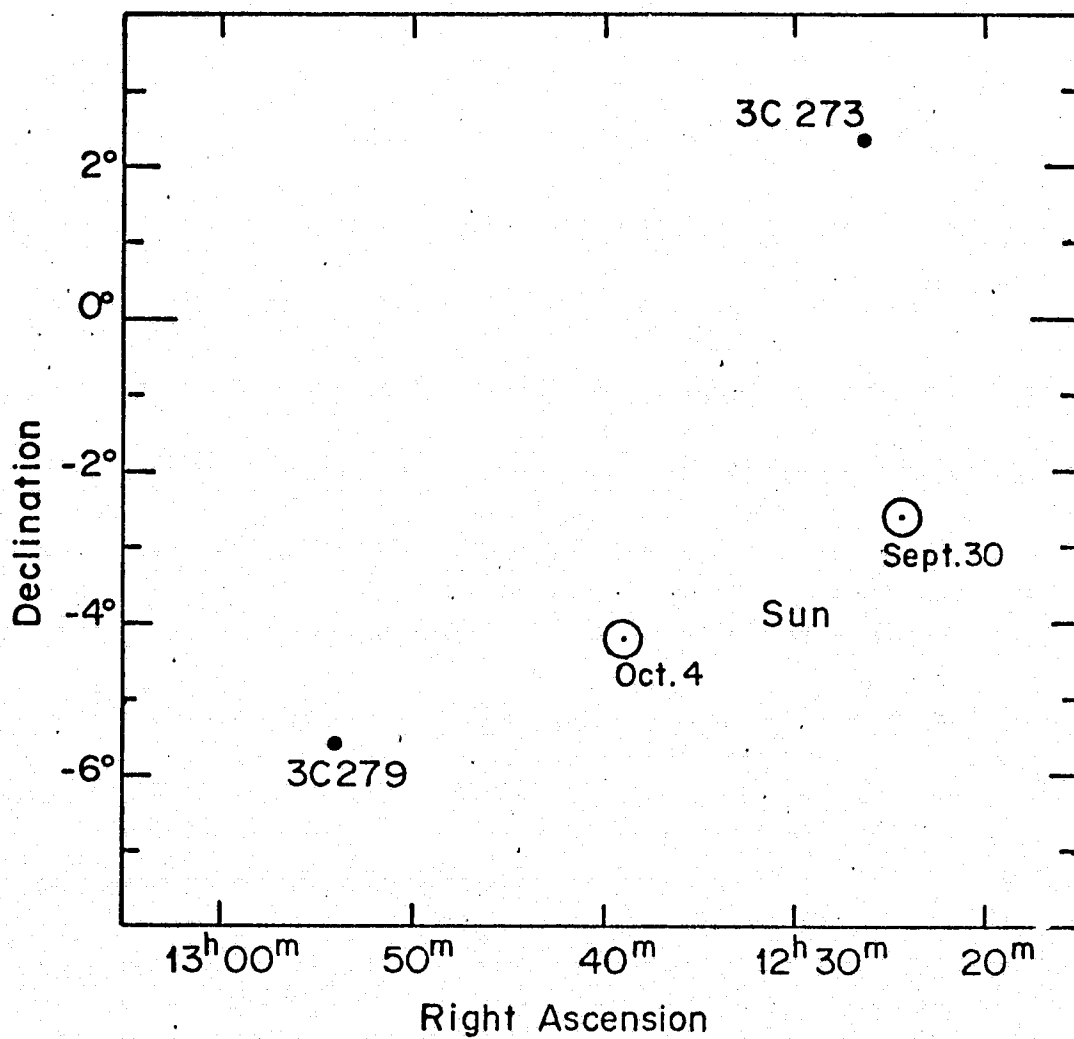sampled.

FIGURE II-3

The source configuration for the VLBI experiment. The position of
the sun on the observing days is shown.

12 f.u., and the relative phases between orthogonal circular polar-
izations were easily measured. On the two days of observations 3C
273 was 5.0 and 7.8 degrees from the sun.

We have not been able to determine the phase difference in
orthogonal linear polarizations due to a discrepancy, as yet not
understood, in fringe rate between antennas A and B (although the
change in baseline was properly taken into account). Two independent
determinations of phase differences in the circular polarizations
were obtained from separate analyses of the fringes produced by
correlating antenna 85-1 with antenna A, and by correlating 85-1
with antenna B. For a source separated into two components, with
angular separation, δ , at position angle A, the fringe phase differ-
ence is

$$\Delta \varphi = \delta[(B_x \sin A - B_y \sin D \cos A)\sin H -$$

$$(B_x \sin D \cos A + B_y \sin A)\cos H + B_z \cos D \cos A] + \text{constant},$$

where H is the hour angle, (α , D) is the source position, and B_x,
B_y, and B_z are the baseline components in wavelengths. For CR
splitting A is the position angle of a line on the celestial sphere
passing through the sun and the radio source, and for CT splitting
A is orthogonal to this line.

Phase differences between the orthogonal circular polariza-
tions were calculated for scans of 15 minutes during the observing
sessions. The data shown in Figure II-4 were fitted to the equation

by the method of least squares. This was done for the B antenna
experiment on October 4 and for the A antenna experiment on both
days. The B antenna was not functioning properly on the first
observing day. The phase diferences for the upper and lower side-
bands have been kept separate, since the exact times of relative
phase determination, and the values of B_x, B_y, and B_z differ
slightly. Also, the data from both days in the A antenna experi-
ment were, in one case, taken together in the same least squares
fit by arbitrarily assuming the splitting to have a $1/b$ dependence
on solar elongation. None of these least squares fits yielded
significant splitting above the error level. Upper limits for all
of these cases were obtained by calculated χ^2 for assumed values of
δ. The upper limits of the splitting corresponding to the 95%
confidence level are given in Table II-1.

As shown in the table, these observations set an upper limit
of ~ 2 m.a.s. for CT splitting at 7.8 $R_{\odot}$, and ~ 3.5 m.a.s. for
CR splitting. At these solar elongations the total bending is
~ 200 m.a.s. Thus, with some ease upper limits to the polarization
splitting have been set at a level which is $\sim 1\%$ of the bending
angle.

C.   Intermediate Baseline Interferometry

In many high resolution position studies intermediate base-
line interferometry is often competetive with or superior to VLBI.

FIGURE II-4

Relative fringe phase between LCP and RCP for 3C 273. Each point
corresponds to approximately 15 minutes of observing. Upper (Δ)
and lower (∇) sidebands are plotted separately. The arbitrary
additive phase constant has been removed.
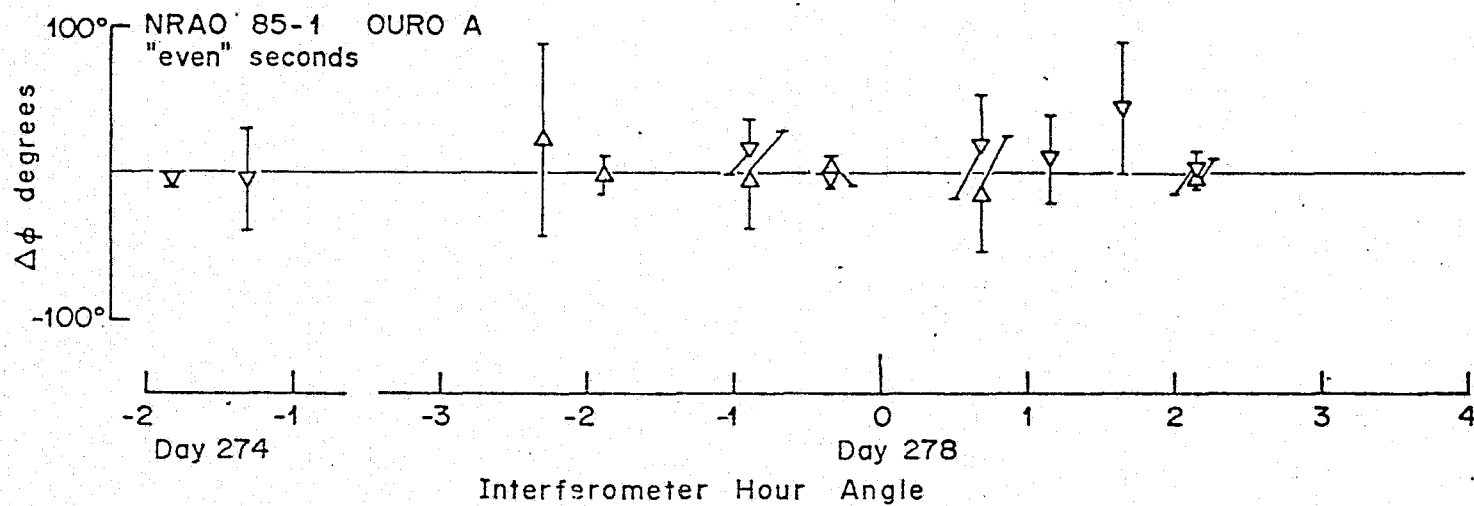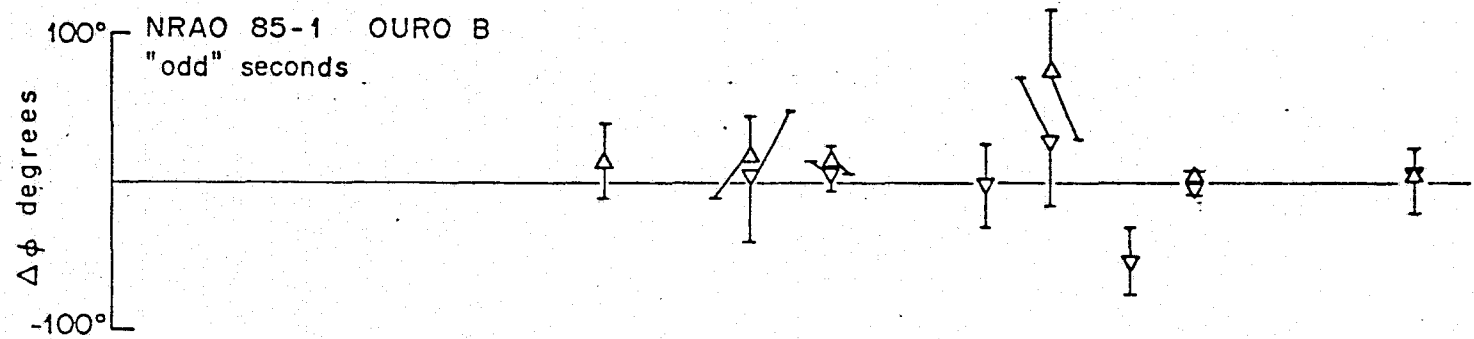
FIGURE II-4

34

TABLE II-1. VLBI Upper Limits to the Polarization Splitting.

Splitting Upper Limits (95% confidence)

- -

Observing days used	Data Used	Solar Elongation $(R_\odot)$	CT (m.a.s.)	CR (m.a.s.)
278	Even	29.	$-2.4 < \delta < 1.9$	$-4.1 < \delta < 3.3$
278	Odd	29.	$-2.2 < \delta < 0.5$	$\delta < 3.0$
274	Even	20.	$-27. < \delta < 25.$	$-336. < \delta < 467.$
274 & 278 no b-dependence	Even	29.	$-2.1 < \delta < 1.5$	$-3.7 < \delta < 3.5$
274 & 278 1/b-dependence assumed	Even	29.	$-1.6 < \delta < 1.1$	$-3.5 < \delta < 3.4$

Positive CT splitting is defined as that seen by an observer in which LCP appears rotated clockwise about the sun away from RCP. In positive CR splitting RCP appears at greater solar elongation than LCP. The "even" data are the result of correlating antennas A and 85-1, and the "odd" data from correlating antennas B and 85-1.

Intermediate baseline experiments have the advantages of larger band-
width and larger correlated flux, and therefore greater signal
strength. For example, compare the intermediate baseline measure-
ments of the light bending (Fomalont and Sramek, 1975, 1976;
Weiler, et al., 1975) with the VLBI studies (Counselman, et al.,
1974). Therefore, intermediate baseline interferometry was used in
a second search.

Fomalont and Sramek (1975) have measured the total bending
of microwave radiation by the sun's gravitational field using the
4-element interferometer of the NRAO. In this section we search for
any polarization splitting based on a separate analysis of their
data. For this, fringe phases in orthogonal circular polarizations
were kindly provided by these investigators. They observed the
three small diameter radio sources, 0116+08, 0119+11, and 0111+02,
at 2695 and 8085 MHz with the 35 km baseline interferometer as the
sun passed close to their line of sight during the period April 5,
1974 through April 17, 1974. Observations were also made when the
sun was out of the field. The geometry of the occulation is shown
in Figure II-5. Observations were also made on March 29 and 30,
and April 24 and 25, 1975 when the sun was out of the field. Numer-
ous other calibration sources were observed to aid in determining
the additive phase constant. Observations on three baselines,
between the 45-foot antenna and the three 85-foot antennas were
carried out simultaneously. Each baseline was about 34 km, or

FIGURE II-5

The source configuration for the intermediate baseline experiment.

The positions of the sun during the observing periods are shown.

The observations were concentrated between April 5 and 17 when the
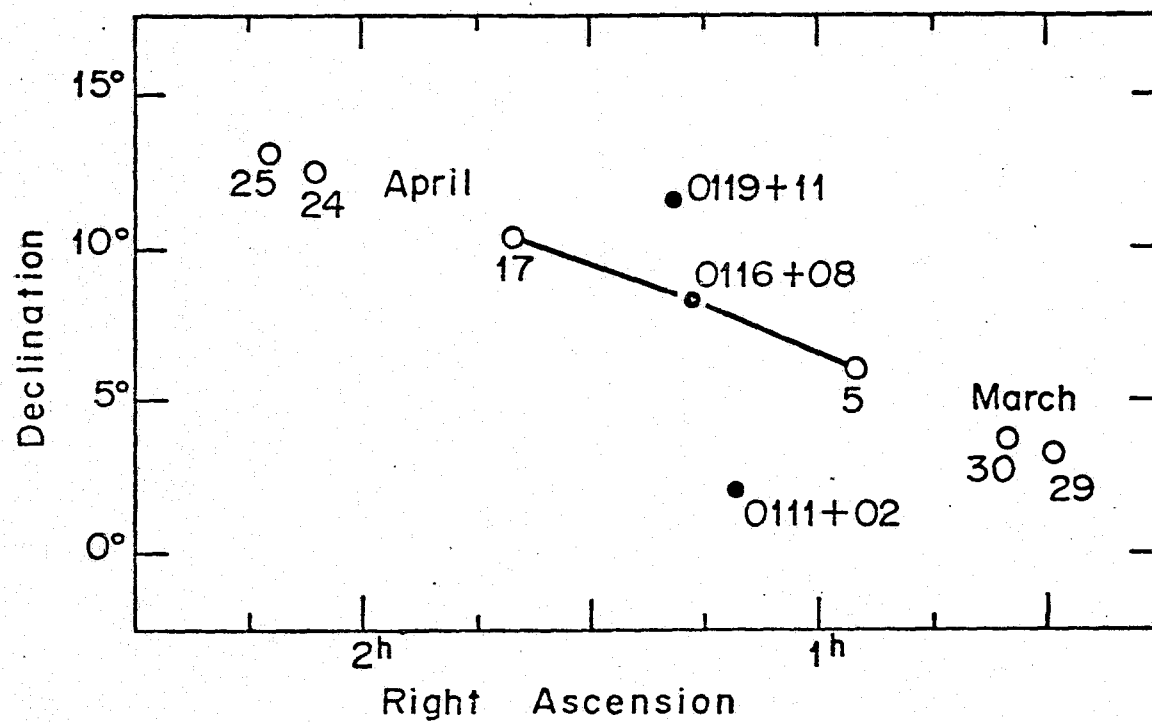
sun passed close to the sources.

FIGURE II-5

nearly 10^6 wavelengths at 8085 MHz.

Although the baseline is nearly two orders of magnitude
shorter than that used in the VLBI measurements, the present experi-
ment has produced improved upper limits to the splitting. This
improvement is attributed to the increased phase stability, in-
creased bandwidth (30 MHz rather than 2 MHz) and correlated flux,
and large quantity of data obtained. For each of three baselines
about 10^3 data points, each representing from 1/2 to 8 minutes of
integration time, were obtained at both frequencies. Also, since
the unresolved source components are considerably stronger, it was
possible to observe sources into smaller solar elongations. The
minimum solar elongations of the observations were determined by
the geometry of the event: 0116+08 was observed to within less than
1 degree of the sun, 0119+11 to within nearly 3 degrees, and
0111+12 to within less than 7 degrees.

The method of analysis was essentially the same as the VLBI
experiment. A finge phase difference of the form,

$$\Delta \varphi = \delta_{(\rho)} \left[(B_x \sin A - B_y \sin D \cos A)\sin H - \right.$$

$$\left. (B_x \sin D \cos A + B_y \sin A)\cos H + B_z \cos D \cos A \right] + \text{constant},$$

was sought. Any angular splitting, $\delta_{(\rho)}$, would be expected to de-
pend on the solar elongation, ρ . Simple power law radial dependence
of the form, $\delta_{(\rho)} = K \rho^{-n}$ (n = 1,2,3) was assumed. Such a functional
form is not inconsistent with the theoretical expectations discussed

in Chapter I. This analysis was necessarily model dependent since
the observations were carried out at numerous elongations.

The above equation was fit to least squares. No polarization
splitting was observed. 95% confidence upper limits were obtained
by calculating χ^2 for various assumed values of K. These upper
limits are given in Table II-2 for both frequencies, for both CT
and CR splitting, and for the different values of n. Since the
three baselines had the smaller 45-foot antenna in common, the three
results were not statistically independent, and in each case the
result with the smallest upper limits was chosen. The upper limits
in Table II-2 are of order 50 - 100 m.a.s. at a solar elongation
of 1 degree. For n ≥ 2 these upper limits represent an improvement
over the VLBI results, when scaled to the same elongation.

D.   Relative Phase Shift Technique

Radiation passing near the sun can be decomposed onto ortho-
gonal components. Consider a wave linearly polarized 45 degrees to
the radial direction. In CR splitting one circular polarization
must suffer a greater phase delay than its orthogonal mode, and
therefore we decompose the wave into LCP and RCP. Reconstructing
the wave at the observer we find a phase difference between these
fundamental modes which produces a rotation of the plane of polar-
ization.

For LR splitting the fundamental modes are linear polariza-
tion aligned radially and tangentially. After differential bending

TABLE II-2

Intermediate Baseline Upper Limits to the Polarization Splitting.

Upper Limits on $K(\rho = 1^{\circ})$ (95% confidence).

n	Frequency (MHz)	CT (m.a.s.)	CR (m.a.s.)
1	2695	- 95. < K < 70.	- 60. < K < 70.
	8085	- 65. < K < 35.	- 50. < K < 30.
2	2605	- 130. < K < 110.	- 75. < K < 95.
	8085	- 70. < K < 90.	- 60. < K < 60.
3	2695	-.195. < K < 165.	- 50. < K < 90.
	8085	- 60. < K < 110.	- 35. < K < 45.

Positive CT splitting is defined as that seen by an observer in which LCP appears rotated clockwise about the sun away from RCP. In positive CR splitting RCP appears at greater solar elongation than LCP.

the phase difference produces the change in polarization shown in Figure II-6. A small phase delay produces a transition to elliptical polarization. When the delay reaches 1/4 cycle the resulting wave is circularly polarized. A 1/2 cycle delay produces linear polarization orthogonal to the initial state. Further phase delay again produces ellipticity but with the opposite sense of rotation. At 3/4 cycle the orthogonal mode of circular polarization is reached. For a full cycle of delay the original polarization state of the wave is reformed. Whether the wave first progresses to LCP or RCP as the delay increases depends upon which fundamental mode suffers the greatest delay.

Initially, we can apply these considerations to existing data of Stelzried, et al. (1970). They observed the polarization of the 13 cm wavelength carrier wave transmitted by the Pioneer 6 spacecraft as it was occulted by the sun. The emitted radiation was polarized perpendicular to the ecliptic. When the line of sight passed within 6 $R_\odot$ of the sun Faraday rotation began, eventually rotating through 135 degrees by 4 $R_\odot$. Ath this point the signal was lost because of solar contamination in antenna sidelobes.

In a single frequency experiment CR splitting cannot be distinguished from Faraday rotation, and upper limits can only be set at those elongations at which no rotation is observed. At $\rho \sim 7$ $R_\odot$ the total delay is $\sim 10^6$ cm. From the lack of large rotation effects at this elongation we can safely assume that the delay, and therefore

43

FIGURE II-6

The polarization of a wave formed by the superposition of two ortho-
gonally polarized waves. The resulting polarization depends on the
phase relationship or delay between the two waves.
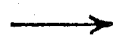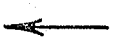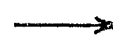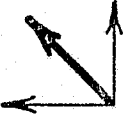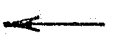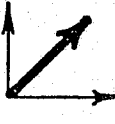
FIGURE II-6

its associated bending, are identical to a part in $\sim 10^5$ for both circular polarizations.

Stelzried, et al. (1970) also sought the development of ellipticity in the signal. However, ellipticity exceeding 0.1 in power, the instrumental resolution, was not detected. At some point during the observations the Faraday effect must have rotated the plane of polarization to 45 degrees at the point of closest approach, producing an even mixture of radially and tangentially aligned linear polarization. The lack of ellipticity implies a phase shift between the linear polarization components $\leqslant 1$ cm. Since the total delay is $\sim 10^6$ cm, any LR splitting must be less than a part in 10^6 of the total bending at this elongation.

We now carefully apply the LR splitting analysis to an experiment which was conducted with the sun-orbiting spececraft, Helios 1. This spacecraft transmits a carrier wave of 13 cm wavelength, with the plane of linear polarization perpendicular to the ecliptic. In April, 1975 and August, 1975 Helios 1 was occulted by the sun. The Helios 1 experiment has the advantages of higher gain in the transmitted signal and lower noise from contamination of the antenna sidelobes by the sun since the sun was near a minimum of activity in 1975.

As discussed previously LR splitting would produce a transition to elliptical polarization in the signal. For this splitting the fundamental modes are aligned radially and tangentially, and

Faraday rotation plays the essential role of rotating the plane of polarization. After $\pm$ 45 degrees of Faraday rotation the signal becomes an even mixture of fundamental modes at which point the maximum gravitational phase shift could occur. Stelzried, et al., (1970) have calculated typical values of the Faraday rotation in a quadrant of the "quiet" sun, and from this we can see that the signal should reach $\pm$ 45 degrees of Faraday rotation at closest· approach somewhere between 4 $R_\odot$ and 7 $R_\odot$. This is consistent with the Helios 1 Faraday rotation data reported by Volland, et al., (1976). The observed Faraday rotation is not a direct measure of the amount of rotation accumulated by closest approach because of the sector structure of the magnetic field (Stelzried, et al., 1970; Volland, et al., 1976). However, the Faraday rotation in a single sector should be of about the same magnitude or larger than the observed Faraday rotation. During the April, 1975 occulation Volland, et al., (1976) observed that the Faraday rotation varied from about 20 degrees to -45 degrees between 7 $R_\odot$ and 4 $R_\odot$; thus at some point in this range the amount of rotation at closest approach should have reached -45 degrees. For elongations $\leqslant$ 4 $R_\odot$ the magnitude of the Faraday rotation grows rapidly as the elongation is decreased.

Using the NASA/JPL 64-meter antenna of the Deep Space Network at Goldstone, California (DSS 14), the Helios 1 carrier wave was monitored for a development of ellipticity on days (of the year)

109-114 inclusive during the April, 1975 occulation, and on days
244-246 inclusive during the August, 1975 occulation. The relative
positions of the sun and spacecraft during the observations is
shown in Figure II-7. A closed loop polarimeter discussed by
Stelzried (1970) automatically tracked the polarization of the
signal, and monitored the signal for ellipticity. The resulting
integrated ellipticity scans are shown in Figures II-8 and II-9.
As the solar elongation decreased the system noise increased due
to the passage of the sun through antenna sidelobes. The ellip-
ticity scans have been averaged with an effective integration con-
stant of about several hundred seconds of observing time, and the
random errors are comparable to the widths of the curves in the
figures. The main limitation appears to be due to the instrumental
polarization which has ellipticity components. Several percent of
systematic ellipticity error may stem from errors in the zeroing of
the ellipticity. The instrumental ellipticity was measured by
carrying out observations on days 96, 97, 100 and 251 when the angle
between Helios 1 and the sun was large (~ 20 $R_\odot$). The instrumental
ellipticity was found to depend on hour angle, and to be reproduc-
ible from day to day. The resulting curves are shown in Figures II-8
and II-9. However, when the main beam is near the sun the curves
vary by up to 8% (maximum), and we attribute this to the passage of
the sun through sidelobes having different instrumental ellipticity,
and possibly to heating of the various parts of the telescope

FIGURE II-7

The positions of the Helios 1 spacecraft relative to the sun during the April (a) and August (b) occulations. Filled circles depict the spacecraft positions during the observing periods. Closest approach during the April, 1975 occulation occurred on day 126. The August, 1975 occulation was complete; the spacecraft passed behind the sun. Scale is in $R_\odot$.

W

E

126

114 113 112   111   110   109

Ecliptic

(a)

246   245   244

Ecliptic

E

W

(b)
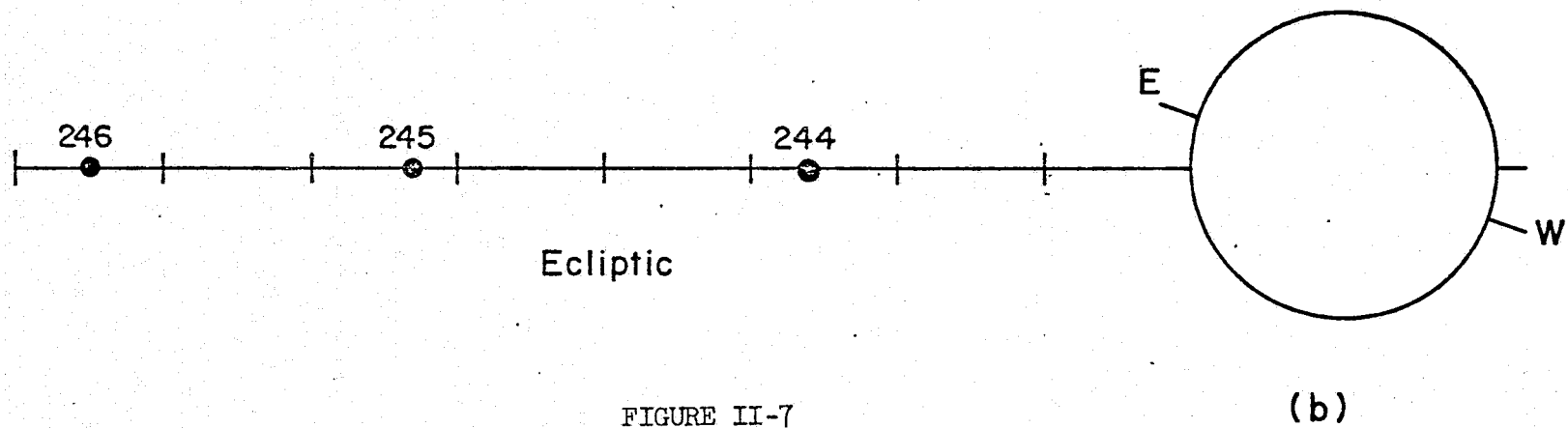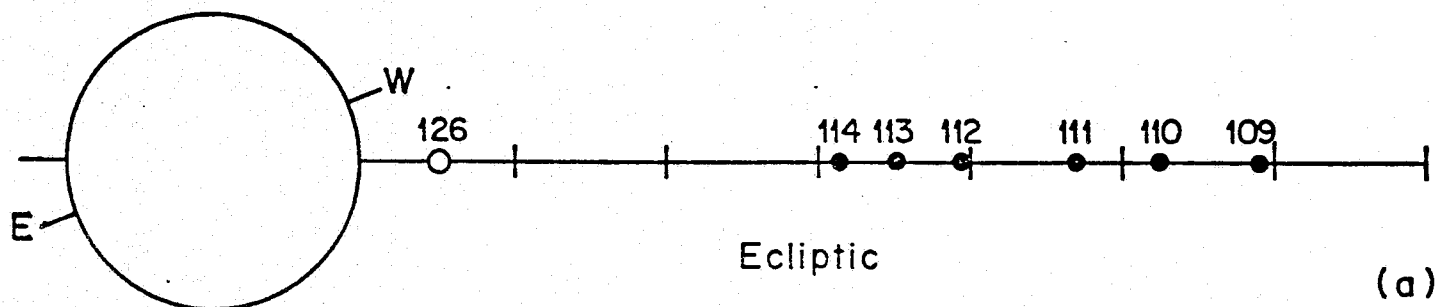
FIGURE II-7

FIGURE II-8

Ellipticity scans obtained during the April, 1975 occulation. The
instrumental ellipticity measured on days 96, 97, and 100 appears
as a solid line. The scans for the observing days appear as follow:
109 (— . — . — ·), 110 (— — —), 111 (·····), 112 (-------),
113 (– ·· – ·· –), and 114 (– - – - –).
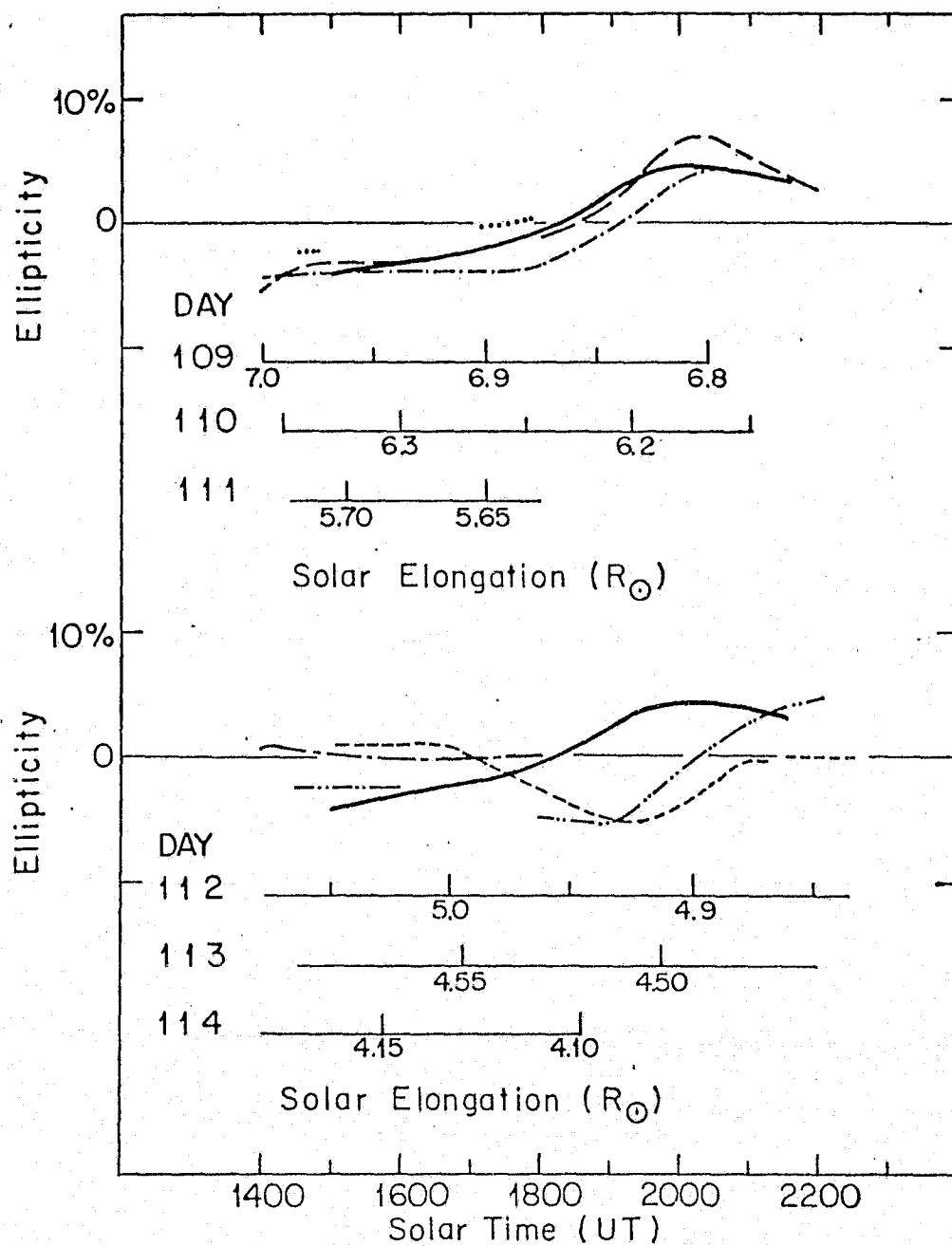
FIGURE II-8
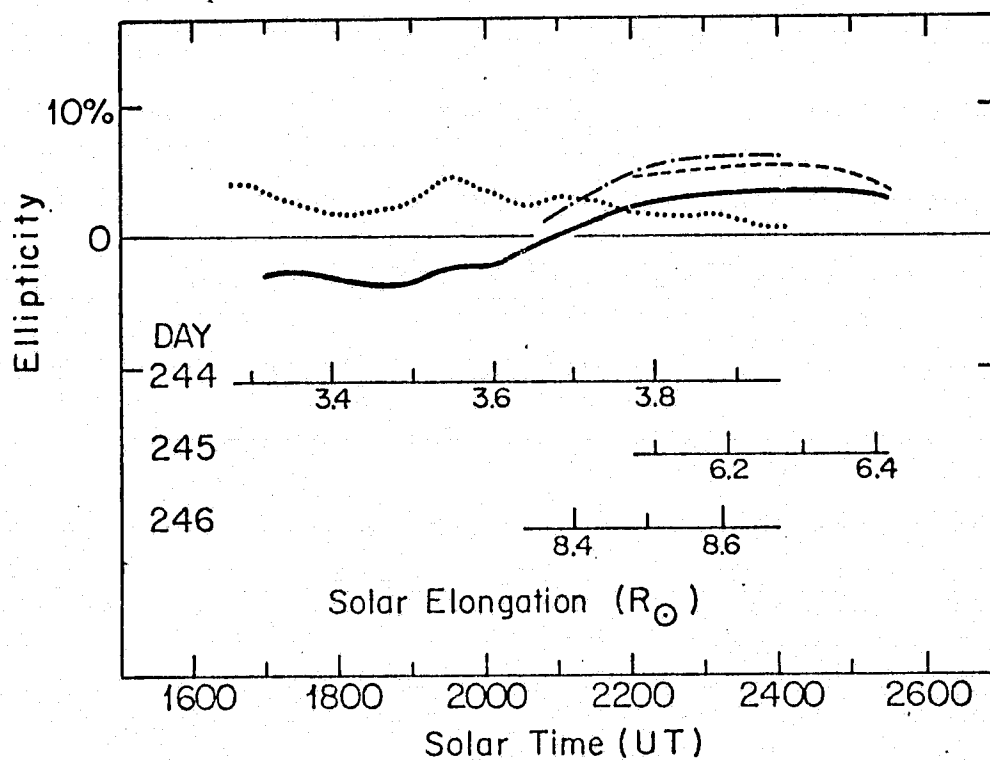
FIGURE II-9

Ellipticity scans obtained during the August, 1975 occulation. The
instrumental ellipticity measured on day 251 appears as a solid line.
The scans for the observing days appear as follows: 244 (········),
245 (------), and 246 (— · — · — ·).

structure. In support of this we observed that the slight increase in ellipticity at 1930 hours on day 244 is associated with a dramatic increase in noise (evident with 1-second integration time), and is therefore explained by the passage of the sun through a side-lobe having substantial instrumental ellipticity. These instrumental effects appear to be the main limitation of this technique.

The data obtained during the April, 1975 occulation cover the elongation range 7 $R_\odot$ to 4 $R_\odot$. In this range Faraday rotation produced optimal conditions for the gravitational phase shift, which would have been of sufficient duration to have been detected during at least one of the observing periods. The observed ellipticity does not deviate from the instrumental ellipticity by more than 0.1 (in power), indicating a maximum shift between orthogonal components of $\sim 1/5$ cm. Since the time delay for a wave passing within 4 $R_\odot$ to 7 $R_\odot$ is $\sim 2 \times 10^6$ cm, then the time delay and therefore the bending should be identical for both linear polarizations to a part in 10^7 of the total bending (at that elongation).

Data taken during the August, 1975 occulation extend our results to a smaller elongation than previously studied. Because of the good signal-to-noise ratio and low solar activity it was possible to observe Helios 1 to as close as 2 $R_\odot$ (Volland, et al., 1976). The circumstances of our observations permitted us to obtain the scan of day 244 covering the range 3.3 $R_\odot$ to 3.95 $R_\odot$. During this scan Volland, et al., (1976) recorded a variation in Faraday rotation

from about -220 degrees to -40 degrees. Sometime during this period optimal condition for the gravitational phase shift must have occurred, yet no signal ellipticity exceeding 0.1 was observed, indicating a phase shift between orthogonal components $\leqslant 1/5$ cm. At this elongation, the time delay is $\sim 3 \times 10^6$ cm, and thus the bending of both linear polarizations are identical to a part in 1.5×10^7 of the total bending.

Levy (1967) carried out a related experiment with the RCP signal of Mariner IV. He sought a development of LCP when the signal passed within 4.2 $R_\odot$ of the sun. LCP was not detected above the 10% level of total signal power. Differential propagation of orthogonal linear polarizations would produce a mixture of LCP and RCP. These results are further confirmation of a lack of radial splitting between linear polarizations at the level of our upper limits. The phenomenon sought by Levy (1967) is based upon a postulated relativistic streaming anisotropy in the solar wind (Lusignan, 1963), and has the same effect as radial splitting between linear polarizations. The Helios 1 data yield no evidence for this streaming effect, and are consistent with the assumption that the electron streaming velocity equals the proton streaming velocity.

The lack of phases shifts in the Helios 1 data implies that the radial difference in bending between orthogonal linear polarizations is less than 5×10^{-5} m.a.s. in the overall range, 3.3 $R_\odot$

to 7 $R_\odot$. By detailed application of the relative phase shift tech-

nique these upper limits are nearly an order of magnitude below those

extracted from the Pioneer 6 data. Also, these results have been

extended to within 3.3 $R_\odot$ elongation.

The upper limits to CR and LR splitting are given in Table II-3.

The CR limits are from the Pioneer 6 data (Stelzried, et al., 1970)

since the Helios 1 Faraday rotation data (Volland, et al., 1976) only

serve to confirm these limits.

The optimum angular resolution achieved by this technique is

quite astounding. Quite straightforwardly we have shown that any

LR splitting must be 7 orders of magnitude smaller than the bending

angle itself.

E.   Conclusions

The best upper limits to the various splittings are given in

Table II-4. At 29 $R_\odot$ CT splitting is less than about ~ 2 m.a.s.

For the various model dependent CT splittings, the splitting magni-

tude at 4 $R_\odot$ (= 1 degree) is less than 50 - 100 m.a.s. CR splitting

is less than ~ 2 x 10^{-3} m.a.s. at 7 $R_\odot$, and LR splitting is less

than ~ 2 x 10^{-5} m.a.s. in the range 3.3 $R_\odot$ - 7 $R_\odot$. Because no

interferometry experiment sensitive to linear polarization has yet

been carried out successfully, upper limits to LT splitting are not

available.

Table II-4 clearly illustrates the domains of the various

TABLE II-3

Phase Delay Upper Limits to the Polarization Splitting

Splitting Upper Limits (95% confidence).

Spacecraft	Solar Elongation $(R_\odot)$	CR (m.a.s.)	LR (m.a.s.)	Reference
Pioneer 6	7	$\lvert\delta\rvert < 2.1 \times 10^{-3}$		Stelzried, et al. (1970) and this
Pioneer 6	4-6		$\lvert\delta\rvert < 2.5 \times 10^{-4}$	work.
Helios 1	3.3-7		$\lvert\delta\rvert < 5 \times 10^{-5}$	This work

TABLE II-4. Established Upper Limits to the Polarization Splitting.

Splitting Upper Limits.

Technique	Model Parameter	Wavelength (cm)	Solar Elongation ($R_\odot$)	CT (m.a.s.)	LT (m.a.s.)	CR (m.a.s.)	LR (m.a.s.)
VLBI	none	3.8	20.	$-27. < \delta < 25.$			
VLBI	none	3.8	29.	$-2.2 < \delta < 0.5$			
VLBI	$n = 1$	3.8	(4.)	$-12. < K < 9.$			
IBI	$n = 2$	3.8	(4.)	$-70. < K < 90.$			
IBI	$n = 2$	11.1	(4.)	$-130. < K < 110.$			
IBI	$n = 3$	3.8	(4.)	$-60. < K < 110.$			
IBI	$n = 3$	11.1	(4.)	$-195. < K < 165.$			
Phase Delay		13.	7.			$\lvert \delta \rvert < 2.1 \times 10^{-3}$	
Phase Delay		13.	3.3-7.				$\lvert \delta \rvert < 5 \times 10^{-5}$

Positive CT splitting is defined as that seen by an observer in which LCP appears rotated clockwise about the sun away from RCP. In positive CR splitting RCP appears at greater solar elongation than LCP. IBI denotes intermediate baseline interferometry.

techniques. For radial splitting the phase delay technique excels.
We also note that VLBI is useful for obtaining an upper limit at a
single elongation, whereas intermediate baseline interferometry
relies on a large number of observations which are usually spread
over a range of elongations. Hence, these results are modelled.
Together these three techniques constitute a balanced search for
polarization dependence in the light bending.

These results constitute a new confirmation of the Equivalence
Principle.

The accuracy of these experiments is not yet sufficient to
test any of the specific splitting mechanisms discussed in Chapter I.
As was stated previously C-, P-, T-nonconservation predicts a CR
splitting of magnitude $\delta \simeq \alpha_2 \ 10^{-8}$ m.a.s. for 13 cm microwaves at
the solar limb. Since α_2 is only known to be $\leqslant 10^3$, physically
interesting limits can be put on α_2 if 10^{-5} m.a.s. accuracy can be
achieved. The LR splitting experiment has approached this level.
The primary limitation in a CR experiment is caused by the Faraday
rotation which mimics the gravitational effect.

PART I

CHAPTER II - REFERENCES

Counselman, C. C., Kent, S. M., Knight, C. A., Shapiro, I. I.,

    Clark, T. A., Hinteregger, H. F., Rogers, A. E. E., and

    Whitney, A. R., Phys. Rev. Letters 33, 1621 (1974).

Fomalont, E. B., and Sramek, R. A., Ap. J., 199, 749 (1975).

Fomalont, E. B., and Sramek, R. A., Phys. Rev. Letters 36, 1475 (1976).

Kellerman, K. I., Clark, B. G., Shaffer, D. B., Cohen, M. H.,

    Jauncey, D. L., Broderick, J. J., Niell, A. E., Ap. J. 189,

    L 19 (1974).

Levy, G. S., in The Superior Conjunction of Mariner IV (by Glodstein,

    R. M., et al.) 49-53 (NASA Technical Report 32-1082, Jet

    Propulsion Laboratory (1967).

Lusignan, B. B., J. G. R., 68, 5617 (1963).

Rusch, W. V. T., and Stelzried, C. T., Radio Science 7, 1131 (1972).

Shapiro, I. I., Phys. Rev. Letters 13, 789 (1964).

Shapiro, I. I., Phys. Rev. Letters 20, 1265 (1968).

Stelzried, C. T., NASA Technical Report 32-1401, Jet Propulsion

    Laboratory (1970).

Stelzried, C. T., Levy, G. S., Sato, T., Rusch, W. V. T., Ohlson,

    J. E., Schatten, K. H., and Wilcox, J. M., Solar Physics 14,

    440 (1970).

Volland, H., Bird, M. K., Levy, G. S., Stelzried, C. T., and Seidel,

    B. L., preprint, 1976.

Weiler, K. W., Ekers, R. D., Raimond, E., and Wellington, K. J.,

Phys. Rev. Letters $\underline{35}$, 134 (1975).

CHAPTER III

THE FUTURE

A.   Solar Experiments

There are two areas in which future work may improve upon
the experiments discussed in Chapter II. Firstly, a measurement of
the LT splitting is sorely needed. This might best be accomplished
by a VLBI experiment involving OVRO at one end, since crossed linear
polarizations are available there.[*]

Seoncdly, the CR splitting measurement could be improved if
the electromagnetic Faraday rotation can be isolated. This may be
possible in a multi-frequency experiment. We now outline how this
may be accomplished.

Firstly, we must calculate an expression for the "graviataional
Faraday rotation" which contains all wavelength dependence. As an
approximation we will assume that the bending occurs in a thin screen.
The line connecting the point of closest approach with the center of
the sun is contained within this plane. Along this screen a phase
delay with gradient, $d\varphi/dr$, is imposed upon the wave. The bending
angle then is

$$\theta = - \frac{\lambda}{2\pi} \frac{d\varphi}{dr} \, ,$$

---

[*]   A repeat of the first VLBI experiment was attempted in October,
1973, but failed because the NRAO local oscillator was set
incorrectly.

where r is the radial coordinate. We postulate a bending of the form,

$$\theta = \frac{4M}{r} \left[1 \pm \left(\frac{X}{r} \right)^{\ell} \right] ,$$

where the $\pm$ sign depends upon helicity. X and ℓ are parameters to be specified by a specific theory. In general $X = X(\lambda)$. Then

$$d\varphi = - \frac{8\pi M}{\lambda} \left[\frac{dr}{r} \pm X^{\ell} \frac{dr}{r^{\ell+1}} \right] .$$

The differential phase difference between orthogonal polarizations is

$$d(\Delta \varphi) = - \frac{8\pi M}{\lambda} 2X^{\ell} \frac{dr}{r^{\ell+1}} .$$

Integrating from infinite elongation, where $\Delta \varphi = 0$, to impact parameter, b, we obtain

$$\int_0^{2\Omega_g} d(\Delta \varphi) = - \frac{8\pi M}{\lambda} 2X^{\ell} \int_{\infty}^{b} \frac{dr}{r^{\ell+1}} .$$

Then

$$2\Omega_g = \frac{8\pi M}{\lambda} \frac{2}{\ell} \frac{X^{\ell}}{b^{\ell}} ,$$

where Ω_g is the angle of rotation of the plane of polarization. The ratio of the splitting to the total bending is just

$$\frac{\delta}{\theta} = 2 \left(\frac{X}{b}\right)^{l} \ . \ \ \text{Therefore, we have}$$

$$\Omega_g \ = \frac{4\pi M}{\lambda} \frac{1}{l} \frac{\delta}{\theta} \ .$$

We note that application of this equation to the data obtained in Chapter II, Section D, gives essentially the same limits on δ. For $l = 0$ the thin screen approximation breaks down and we must compute the continual bending as the wave progresses through the medium.

We now compare this to the electromagnetic Faraday rotation in which $\Omega_{e-m} \ \alpha \ \lambda^2$. In principle the electromagnetic Faraday rotation can be separated from the gravitational effect for <u>any</u> theory in which δ/θ is not proportional to λ^3. All of the theoretical effects discussed in Chapter I have $\delta/\theta \ \alpha \ \lambda$, and thus for these effects Ω_g is independent of wavelength. Multi-wavelength observations of a linearly polarized source occulted by the sun could be used to greatly improve the CR upper limits.

Mashhoon (1975) has also analogized the gravitational effect with propagation in a magnetoactive plasma.

B.   Compact Objects

All of the effects discussed in Chapter I become much larger whenever radiation is scattered by compact objects. Mashoon (1973) has shown that in the framework of general relativity radiation scattered by a Kerr black hole should in general be polarized. If

the wavelength is much shorter than the mass, M, then the scattering cross section is $\sim 4\pi M^2$. However, black holes of stellar mass can not effectively eclipse any background source since the cross section is of order $\sim 10 - 1000$ km^2. Mashhoon (1973) has also consiered a binary system consisting of a visible star and a Kerr black hole. He finds that gravitational scattering of starlight from the black hole can dominate over Thompson scattering if the electron density around the black hole is $\leqslant 10^{18}$ cm^{-3}, a reasonable possibility.

If black holes do indeed exist they seem to manifest themselves by the radiation emitted by matter falling into them. Much of this radiation is emitted fairly close to the Schwarzschild radius. A worthwhile question is whether this radiation would appear polarized when viewed by an outside observer in a particular direction. For example, preferential capture of particular polarizations may bring this about for some directions. This question is not easily answered, and depends on the geometry of the emitting region. Also, the polarizing effects of electromagnetic scattering (Lightman and Shapiro, 1975), and interaction with a magnetoactive plasma must be accounted for.

C.   "Large Scale" Compact Objects

To avoid the problem of small cross section, we turn to black holes of much larger mass. This is the only way in which

black holes can subtend an appreciable solid angle, and this may offer some hope in searching for the subsequent polarization of background radiation.

Mashhoon (1974) has calculated the effect that a critical cosmological density of Kerr black holes would have on the 3 degree background radiation. The resulting polarization of the background radiation increases linearly with the mass of a black hole. For mass in the range $10^8 - 10^{11} M_\odot$ he concludes that the polarization is probably negligible.

Now we speculate that the "missing mass" of clusters of galaxies resides in maximally rotating Kerr black holes. Let there be N black holes per cluster, and the missing mass of a cluster be M_d. The gravitational scattering cross section per black hole is $4\pi M_d^2 N^{-2}$. The total cross section is $4\pi M_d^2 N^{-1}$. Taking the optimum case of a single black hole binding the cluster, then we may hope to see some polarization of the 3 degree background radiation over a solid angle

$$\Omega_p \sim 4\pi \frac{M_d^2}{\ell^2} ,$$

where ℓ is the distance to the black hole. If this effect is observed with a telescope with beam solid angle, Ω_b, the polarized flux is diluted by the factor Ω_p/Ω_b. As an example, we consider the 36-foot radiotelescope of the NRAO. At 85 GHz the beam size is

$\sim 1'$. Two possible examples are given in Table III-1.

This would be difficult to observe. It is not known to what extent the flux is polarized over Ω_p, and of course, this becomes severely diluted by the observational resolution. Interferometric observations sensitive to polarization structure with scale $\sim 1/2$ arc sec may offer some hope. Fortunately, only the dynamical center of the clusters need be searched, since $M_d \gg M_{luminous}$. However, with a small beam this may still involve numerous beam areas.

Finally, we consider the largest scale object which is still "compact" in the gravitational sense, the universe. Mashhoon (1975) has calculated the splitting of a distant image into orthogonal circular polarizations in a Gödel universe. In such a cosmology the universe can be thought of as rotating, and this anisotropy gives rise to a separation of electromagnetic radiation into opposite helicity states. At present, the isotropy of the 3 degree background radiation severely limits the rotation of the universe, and this constrains the image splitting to be smaller than that which is presently detectable.

D.   Conclusions

There is still room for some improvement in solar experiments. An LT splitting measurement is needed, and eventually it may be possible to improve the CR measurement. When more is known about

TABLE III-1

Polarization of the Background Radiation
by Large Kerr Black Holes.

- -

Cluster	M_d (Mpc)	ℓ (Mpc)	Ω_p/Ω_b
Coma	10^{-4}	10^2	2×10^{-4}
Virgo	3×10^{-5}	10	2×10^{-3}

the physics of compact objects much more stringent measurements may
be possible. In some situations we may expect to observe nonzero
polarization dependent effects.

PART I

CHAPTER III - REFERENCES

Lightman, A. P., and Shapiro, S. L., Ap. J. Letters 198, L73 (1975).

Mashhoon, B., Phys. Rev. D. 7, 2807 (1973).

Mashhoon, B., Phys. Rev. D. 10, 1059 (1974).

Mashhoon, B., Phys. Rev. D. 11, 2679 (1975).